Journal Pre-proof

PyShoreVolume 1.0.0: A Python based Shoreline Change and beach Volumetric Change Analysis tool

Owen C. James, Daniel N. Schillereff, Stuart W.D. Grieve, Andreas C.W. Baas

PII: S0098-3004(24)00074-8
DOI: https://doi.org/10.1016/j.cageo.2024.105591
Reference: CAGEO 105591

To appear in: *Computers and Geosciences*

Received date : 18 July 2023
Revised date : 15 December 2023
Accepted date : 2 April 2024

Please cite this article as: O.C. James, D.N. Schillereff, S.W.D. Grieve et al., PyShoreVolume 1.0.0: A Python based Shoreline Change and beach Volumetric Change Analysis tool. *Computers and Geosciences* (2024), doi: https://doi.org/10.1016/j.cageo.2024.105591.

Highlights

PyShoreVolume 1.0.0: A Python Based Shoreline Change and Beach Volumetric Change Analysis Tool

Owen C. James 1,Daniel N. Schillereff 2,Stuart W.D. Grieve 3,Andreas C.W. Baas 4

- A new Python based Shoreline Change and Volumetric Change Analysis tool for rapid, accurate coastal change assessments.
- Performs five well established Shoreline Change Analysis functions producing map based graphics of shoreline change and a Pandas Dataframe of results.
- Functions perform rapid, automated, reproducible Volumetric Change statistics and graphics to be produced across a time series or for particular seasons.
- Shoreline Change Analysis function outputs correlate near perfectly with well established toolkits AMBUR and DSAS ($R > 0.97$, $P < 0.001$)
- Functionality and performance of PyShoreVolume demonstrated by capturing coastal sediment dynamics at the Taw and Torridge Estuary, North Devon, UK.

PyShoreVolume 1.0.0: A Python Based Shoreline Change and Beach Volumetric Change Analysis Tool

Owen C. James 1[a], Daniel N. Schillereff 2[a], Stuart W.D. Grieve 3[b] and Andreas C.W. Baas 4[a]

[a]Department of Geography, King's College London,40 Bush House ,North East Wing, Aldwych, London WC2B 4BG
[b]School of Geography, Queen Mary's University London, Mile End Rd, Bethnal Green, London E1 4NS

ARTICLE INFO

Keywords:
Shoreline Change Analysis
Volumetric Change Analysis
Accretion
Python
Erosion

ABSTRACT

Shoreline Change Analysis (SCA) and Volumetric Change Analysis (VCA) are of growing importance to coastal managers throughout the world. The volume, resolution and accuracy of shoreline configurations are gradually improving, which demands tools for efficient processing and analysis. The limited number of systems that combine the two analysis types have lengthy workflows or require commercial software licences, with no current tool that automates VCA from a time series of Digital Elevation Models (DEM's). We present a new, dedicated and open-source package for automating SCA and VCA in the Python environment. It is designed with a user-friendly interface and workflow, delivers efficient processing speeds, automatically generates map based graphical outputs and computes a full range of positional statistics. We verify the package delivers equivalent outputs to existing tools (AMBUR, DSAS) and demonstrate strong performance by reconstructing erosion and accretion over the last twenty years along the beaches of the Taw and Torridge Estuary, North Devon, UK, a region known to have a complex sediment and morphometric dynamics.

CRediT authorship contribution statement

Owen C. James 1: Package code creation and development, morphological analysis and manuscript drafting. . **Daniel N. Schillereff 2:** Package design and manuscript drafting. **Stuart W.D. Grieve 3:** Package development and manuscript drafting. **Andreas C.W. Baas 4:** Manuscript Drafting.

1. Introduction

Shorelines are valuable natural assets that provide economic services through coastal protection and recreation while supporting important ecological habitats (Burvingt et al., 2017; Luijendijk et al., 2018; Paola et al., 2023). Shoreline position and morphology of the subaerial beach zone are subject to numerous interacting forcings. Wave parameters (Direction, Height, Period) and tidal currents drive sediment transportation in cross and long shore directions (Aagaard et al., 2004; Stive and de Vriend, 1995), estuarine and fluvial depositions supply sediments to coastal systems (Roy et al., 1995) while geological constraints dictate the sediment types being provided and ways in which hydrographic variables interact with the intertidal zone (Jackson et al., 2005). Climate change is projected to drive sea-level rise globally with regional storm models projecting higher intensity storm activity across the UK, increasing susceptiblity to inundation and erosion (Griggs and Reguero, 2021). Anthropogenic pressures such as sand dredging can exacerbate coastal vulnerability by reducing how well beaches recharge sediment stores, while coastal defences can enhance erosion down drift of the structure through alterations to sediment supply (Leafe et al., 1998;

ORCID(s): 0000-0000-0000-0000 (O.C.J. 1)

Burningham and French, 2017; Burvingt et al., 2017; Balaji et al., 2017). Assessing current and historical behaviours of the shoreline is critical for coastal managers to better predict areas prone to higher rates of change, allowing site specific management strategies to be developed and implemented (Burningham and Fernandez-Nunez, 2020).

Shoreline Change Analysis (SCA) and Volumetric Change Analysis (VCA) are computational techniques to efficiently quantify sediment movement and transport rates along shorelines. Outputs are widely used to better understand areas most at risk, determine rates of change and pinpoint key drivers of erosion and accretion (Jackson et al., 2012; Pollard et al., 2019). Both techniques have been utilised since the 1970's with a range of well established metrics and statistical descriptors being consistently used by coastal scientists (Burningham and French, 2017; Burningham and Fernandez-Nunez, 2020; Carvalho et al., 2021; Grilli and Horrillo, 1970; Morton, 1975; Pollard et al., 2019). However, there are surprisingly few computational packages to perform SCA and VCA. The most well established is ArcGIS DSAS, which provides a GIS-based workflow to calculate SCA metrics (Himmelstoss et al., 2021). Costs of a professional ArcGIS license may restrict usage of this approach. Open source options include the Analysing Moving Boundaries in R (AMBUR) tool, and the QGIS based EPR4Q, and the Python based Coastsat (Jackson and Short, 2020; Vos et al., 2019). Each generate SCA statistics, but require considerable manual user input and do not automate satellite image based outputs, and in the case of Coastsat can only map changes of 10 meters or above. Methods to perform VCA are limited to manual processing within GIS or programming environments, or in the case of the Geomorphic Change Detection Software a stand alone toolkit that has Python and Matlab back ends (Wheaton et al., 2010). GIS based methods involve clipping, masking and volumetric calculations on each individual dataset in the series. At present, no computational tool provides the functionality to perform SCA and VCA in a highly automated manner with minimal precursor user expertise and input required. This paper presents and evaluates the performance of a new open-source Python package that achieves these objectives -'PyShoreVolume'. The tool extracts key SCA metrics from shapefiles created after a short QGIS workflow and computes VCA metrics wherever time series of DEMs are available for a given beach. Our package is efficient, largely automated, user-friendly for non-computational experts, and promotes the use of publicly available data in the rapid assessment of coastal change.

2. Design and Methodology

SCA can be defined as the analysis of shoreline positional changes at set points throughout time (Burningham and Fernandez-Nunez, 2020). The most common practice is for shorelines to be extracted from maps or geospatial data that span months or years through georeferencing and vectorisation (Burningham and Fernandez-Nunez, 2020). This produces a time series of shoreline polylines from which a range of metrics can be computed, reflecting the distances between shoreline extents at different moments in time. These metrics provide a means by which to assess rates of change and their trends, identify if a shoreline is stable or experiencing erosion or accretion, and what the yearly

positional changes are expected to be. The most widely used metrics are Linear Regression Rate (LRR), Shoreline Change Envelope (SCE), Net Shoreline Movement (NSM) and End Point Rate (EPR) (Burningham and Fernandez-Nunez, 2020; Himmelstoss et al., 2021; Morton, 1975). The approach is usually performed using cross-shore transects set at specified intervals along the selected coastal area. Intersections between the transect and each shoreline is extracted to produce coordinates of each shore point which can then be used for distance measurements (Burningham and Fernandez-Nunez, 2020).

VCA assesses the volumetric differences across the entire subaerial zone rather than the positional changes of a chosen shoreline indicator. This technique requires a time series of rasterised elevation models over the region in question that identifies the elevations of each pixel above ordnance datum, known as a DEM. Each consecutive DEM is subtracted from the former allowing elevation changes of each to be pixel calculated, as shown in Equation 1 (Gares et al., 2006):

$$DOD = DEM_{new} - DEM_{old} \tag{1}$$

Where DEM_{old} is the older DEM and DEM_{new} is the more recent in the series, and DOD is the Digital Elevation Model of Difference product. Volume is then calculated as the elevation changes per pixel multiplied by the pixel area summed across the whole DOD (Gares et al., 2006):

$$V = \Sigma_{i=1}^{i=n} Z_i * A_i \tag{2}$$

Where Z_i is the value of the DOD pixel, and A_i is the area of each pixel. Error can be integrated into the total volumetric change calculations through the exclusion of DOD pixel values that fall within the maximum vertical error found in metadata of the timeseries of DEM files. This process, known as Limit of Detection (LOD), provides volumetric measurements which exclude DEM instrument errors. At present only the Geomorphic Change Detection software provides the functionality to easily integrate error into ranges into software outputs (Wheaton et al., 2010). To allow comparison between between beaches the volume change per unit beach width in m^3 (QNet) is calculated by normalising the DOD by the beach length, where L_s in the length of the beach in meters (Burvingt et al., 2017).

$$QNet = 1/L_s \Sigma_{i=1}^{i=n} Z_i * A_i \tag{3}$$

The gross cross shore volumetric change (Qgross) is calculated as the sum of the absolute value of volumetric change normalised by the length of the beach, L_s (Burvingt et al., 2017).

$$QGross = 1/L_s \Sigma_{i=1}^{i=n} |Z_i * A_i| \quad (4)$$

The PyShoreVolume package is designed to efficiently perform both set of analytical techniques. It aims to provide the users with the capability to perform a range of SCA functions after a limited amount of pre-processing in open source GIS environments such a QGIS (QGIS, 2023) and the first VCA functions that automate the production of DODs, significantly reducing the required computational time. This paper focuses on the package's functionality and performance. Users are referred to the GitHub repository where a guide to the initial pre-processing is provided in the 'README' documentation, to create the shoreline shapefile required for the intersection extraction. Additional PyQGIS scripts are provided to create the series of DEMs required for the VCA analysis. In brief, it merges all files in a series of folders named in 'YYYYMMDD' format containing '.asc' files from the study region to create a combined DEM of the region per date of survey. From this the shoreline shapefile required for the intersection extraction and the series of DEMs required for the VCA analysis is obtained.

2.1. Cleaning and Configuration

Initially, data cleaning and definition protocols need to be set using the Clean and Transect Locator class. This class has 6 input parameters - Intersects shapefile, Transects shapefile, Path to data directory, Coordinate Reference System, list of Georeferencing errors, and a list of Measurement errors. In this context measurement error is the accuracy range of the instrument used to collect the data, whilst georeferencing error refers to the error range between the coordinates of data points on a map or image and its actual location on a ground system (Bloom et al., 2018; Kim and Meissner, 2017; Hackeloeer et al., 2014). The two lists of errors need to be provided in a python list, in order from youngest to oldest shoreline where they are then assigned to each shoreline date in a new DataFrame column. Table 1 shows each function, its output and a description of its purpose.

2.2. Shoreline Change Analysis Functions

Each key SCA metric can be computed using PyShoreVolume (Table 2) (Burningham and Fernandez-Nunez, 2020). The intersect file is required to have a field called 'layer' filled with the date of the shoreline vector in 'YYYYMMDD' format, and a field called 'TR_ID', which defines the transect id number. The use of GeoPandas allows the coordinates of each shapefile attribute to read into a 'geometries' column (Jordahl et al., 2020).

Table 1
Configuration and Cleaning Functions

Function	Description	Output
transectstartlocator1/ transectstartlocator2	Locates the starting point of the transects from the seaward baseline and merges them into the intersect shapefile. When the transect files are read the coordinates are occasionally read as the transect end points not the starting points and thus the model will interpret the baseline to be on the land causing incorrect erosion and accretion rates to be calculated. A plot of the transects extracted will show if the correct coordinates have been chosen - if incorrect coordinates, use transectstartlocator2 function.	GeoDataFrame with Transect baseline coordinates merged using the associated transect ids.
cleaning	Removes any duplicate shoreline intersects if one has already been read closer to the baseline. Removes any transects where shorelines intersections have not been identified allowing for gaps in the shoreline from streams or paths to be ignored.	Cleaned intersection GeoDataFrame.
errors	Adds the georeferencing and measurement errors to each specified shoreline date, passed to the function in the form of a list of errors ranging from oldest to youngest allowing error ranges to be calculated in the End Point Rate method.	Extra columns on the output intersect dataframe.
results	Creates a results folder where all outputs outputs are saved, provides a path name to be used within the other SCA functions	Results folder and path name to the results folder.
errors	Assigns measurement and geo-referencing error column associated with each survey to intersection dataframe.	Additional measurement and geo-referencing errors columns.

The SCA function setup is defined by setting each class variable and saving it as an instance of this configuration. A total of 8 variables need to be defined: Coordinate Reference System (CRS), Ellipsoid Model (Ellipsoidal), distances between transect numbers to be plotted on the graph (transectplot), results folder path (save_to_path) and Intersection shapefile (intersectnew). Once the instance of this model configuration is created the full suite of SCA methods can be performed. The output of the results method in the cleaning and configuration class is the path which is required to be input as the 'save_to_path' class variable. Results of each SCA function are saved as a Python dictionary to a results folder created in the results method of the Cleaning class and can also be saved within the Python IDE to a variable namespace as a Pandas DataFrame (Pandas development team, 2023). The map based graphic outputs produced in the SCE, NSM and Net Shoreline Movement Erosion and Accretion (NSMEandA) functions (Table 2) utilises the Contextily package to retrieve satellite map tiles of the region in question, while distance measurements are performed using the GeoPy package distance functions (Arrabas-Bel, 2020; Esmukov, 2022).

Table 2
Shoreline Change Functions

Function	Description	Output	Citation
EPR (End Point Rate)	Rates of change between oldest and newest shore position divided by the length of time between the two, producing graphical output of the results.	Dictionary of EPR values per transect, graphical output of the EPR rates per transect with error bars, Pandas DataFrame of Statistics.	(Morton, 1975).
LRR (Linear Regression Rate)	Fits a linear regression model to the change of each shoreline position along a given transect throughout time. Allows for regression statistics to be used to assess positional trend and the confidence levels of this trend.	Linear regression graphs per transect, Dictionary of Linear Regression statistics, Pandas DataFrame of Statistics.	(Burningham and Fernandez-Nunez, 2020).
SCE (Shoreline Change Envelope)	Maximum distances found between any of the shorelines.	SCE with graphical output of SCE rates on top of satellite Imagery, Dictionary of SCE rates, Pandas DataFrame of Statistics.	(Burningham and Fernandez-Nunez, 2020).
NSM (Net Shoreline Movement)	Net movement between the oldest shoreline position and most recent shoreline position.	NSM with graphical output of NSM rates on top of satellite Imagery, Dictionary of NSM rates, Pandas DataFrame of Statistics.	(Morton, 1975).
NSMEEandA (Net Shoreline Movement Erosion and Accretion)	Net movement between the oldest shoreline position and most recent shoreline position with color coded output for erosion and accretion transects.	NSM with graphical output of NSM rates on top of satellite Imagery, Dictionary of NSMEandA rates, Pandas DataFrame of Statistics.	(Morton, 1975).

2.3. Volumetric Change Analysis

The DOD functions are designed to produce elevation and volumetric change assessments of a chosen beach where there is a time series of DEM GeoTiff files. The structure is the same as the SCA functions, where configurations are set up within a DOD class object and the configuration parameters are set as variables within the class. Eleven variables need to be defined: Sub Plot Columns (subplotcols), Title Size (titlesize), Pixel Size (pixelsize), Coordinate Reference System (CRS), Figure Width (figwidth), Figure Height (figheight), Path to results folder (save_to_path), Path to data directory (path), CRS for Masking Meta Data (MaskingCRS), Data Measurement Error (meters) (measurement error) and Beach Length (beachlength). Table 3 summarises the range of VCA functions available and their given outputs.

For the functions to work correctly the DEMs must be saved as a .Tiff file and needs to be named after the year and month of data collection using the 'YYYYMMDD' naming convention. Initially the Tiff files need to be cropped and masked using the masking function. This requires a pre-made shapefile polygon to define the exact research area. Any pixels outside of the defined polygon region are masked and the newly made Tiff is saved into the directory with '*masked.tif' naming convention. These masked files are used within the rest of the analysis.

Each .Tiff file must have the same resolution per pixel and CRS for accurate subtractions to be made. The functions are designed to allow automated production of DODs even when there is varied data availability over the region in question. The approach crops DEMs to the size of the smaller file in the calculation by extracting the perimeter of the smaller DEM and using this perimeter to crop the other DEM in the calculation. This means that only regions that share spatial coverage between DEMs are used to calculate the volume, reducing the error of the overall volume calculations. An added feature is water or 'zero' value masking. Within the littoral zone, rockpools and streams are abundant. Where DEMs are derived from instruments such as Lidar, measurements over water can not penetrate to the substrate beneath and end up providing these pixels a value of '0'. If the same pixel(s) area is dry in a subsequent DEM in the series then the product DOD will be significantly skewed. The decision was taken to mask any '0' value from the DEMs to avoid resulting erroneous volumetric calculations.

Also provided in the package is an independent oceanographic plot function which allows oceanographic data across the time series of DEMs to be plotted in unison with the volumetric outputs from the DOD functions. The function allows wave period, height and direction to be plotted and calculates monthly averages of each variable. It allows the user to perform analysis on the effects that oceanographic variability has on erosion and accretion events.

3. Initial Testing and Validation

The SCA measurement functions in PyShoreVolume were evaluated against the AMBUR and DSAS tools. The performance of PyShoreVolume against AMBUR was tested using the shoreline data and transect shapefiles supplied in the AMBUR release paper, from Jekyll Island, Georgia, USA (Jackson et al., 2012). The intersection shapefile was created by importing both shoreline and transects into QGIS, extracting the shore position on each transect using the 'intersection' tool and saving the output to the data directory. To allow the PyShoreVolume to function correctly, the 'layer' and 'TR_ID' fields were added to the intersection file manually post creation. The results of Net Shoreline Movement, End Point Rate, Shoreline Change Envelope and Linear Regression Rate were compared between both tools. The distance and EPR results show a strong positive correlation across each metric, with Pearsons Correlation and Independent T-Test assessments showing near perfect comparability (Figure 1). The DSAS test used data downloaded from the Plymouth Coastal Monitoring Center website and primary sourced Lidar derived DEMs of a segment of shoreline on Saunton Sands, Devon, UK (Plymouth Coastal Observatory, 2022). The data was processed

Table 3
Digital Elevation Models of Difference Functions.

Function	Description	Output
Masking	Crops the DEMs using prior made vector shapefile and masks regions outside of the desired area to set data value.	Masked DEMs saved in the chosen directory with the name 'YYYYMM-masked.tif'
DEMofDifference	Identifies the masked DEMs in directory and iterates through them in order from youngest to oldest creating elevation models of difference. Allows DEMs of different sizes within the calculation by cropping the larger DEM to the size of the smaller then performing the difference.	Series of elevation difference models along with model of difference graphs with color scale for change rates. Net and Gross cross shore volumetric change, total volumetric change and LOD volumetric change statistics produced in pandas DataFrame.
OldesttoNewset	Creates a DEM of difference between the oldest DEM and Newest DEM providing elevation change rates across the entire period.	Digital Elevation Model of Difference with graphical production with color scale for elevation change rates.
NetVolumeChange	Applies the pixel size parameter to the elevation models to calculate volumetric changes using the Oldest to Newest DEMoD.	Volumetric changes within and outside of limits of detection.
Seasonal DOD: winterDOD, autumnDOD, springDOD, summerDOD	Allows user to perform analysis on DEMs that fall within the same season. It allows an assessment of the impacts that seasonal conditions may have over elevation and volumetric change rates. Currently seasons are defined for the Northern hemisphere.	Digital Elevation Model of Difference for DEMs that share seasons with graphical production including color scale for elevation change rates.
DODSubplot	Creates one single subplot figure of all Digital Elevation Models of Difference created in the DEM of Difference function.	A combined subplot of elevation of difference models.
OceanographicPlot	Creates a four panel time series plot of Wave Period(s), Height(m),Direction(d) and Volumetric changes. Wave parameter monthly averages are calculated and plotted. User can add survey dates to be plotted as red hashed lines.	A mutipanel time series of wave conditions and volumetric changes.

following the workflow provided in the 'README' documentation with the same intersections being used in DSAS and PyShoreVolume systems. Equivalent Pearson's Correlation Coefficient and Independent T-Test outputs were returned (Figure 2).

Performance testing of PyShoreVolume DOD calculations were assessed against manual processing within QGIS using masking tools and the built in raster calculator (QGIS, 2023). The DEMs used are from Saunton Sands, North Devon, created from Lidar point clouds and sourced from the Plymouth Coastal Observatory over the dates 01/02/2007 and 01/04/2008 (NNRCMP, 2022). Within both QGIS and PyShoreVolume the DEMs are cropped using a polygon shapefile that covers the low water mark up to the vegetation line. Pixels with a value of zero were masked and given

Table 4
Bideford Bay Monthly Average Wave Conditions (NNRCMP, 2023)

Month	Wave Height (Hs (m))	Wave Period (Tp(s))	Direction (Degrees)
January	1.63	11.4	282
February	1.67	12.1	281
March	1.18	11.5	280
April	0.89	10.4	281
May	0.9	9.5	280
June	0.83	8.9	279
July	0.82	8.3	282
August	0.91	8.2	281
September	0.98	9.5	283
October	1.18	10.1	282
November	1.57	10.8	283
December	1.71	11.2	282

'no_data' values to exclude them from the subtracting process through use of the GDAL translate tool. The masked DEMs are then subtracted using the raster calculator, with the output being saved as a .Tiff file. Both output DOD .Tiff files from QGIS and PyShoreVolume are imported into Numpy array using the Rasterio package (Gillies, 2023; Python, 2023). Figure 3 shows the identical positive relationship between the results of both systems and perfect correlation coefficient scores. It is worth noting that the PyShoreVolume tool reduced the processing time significantly due to the automated production of DOD DEMs across the time series.

4. Example Site Assessment

4.1. Study Site

The scope for the PyShoreVolume toolkit to provide critical insight on shoreline dynamics to coastal managers was assessed at the open coast beaches of Saunton Sands and Northam Burrows which form part of the Taw and Torridge Estuary, North Devon, UK. The region is comprised of two beaches which are split by the Taw and Torridge channel (Figure 4). The northern intertidal area is comprised of the 5.5km long Saunton Sands beach backed by the Braunton Burrows dune system, and in the south the 2.8km long Northam beach which is backed by the Northam burrows dune system and golf course. Both beaches have a 400-700 m intertidal zone, with a series of semi exposed swash sand bars, known as the Bideford bar located in the estuary channel (Pethick, 2007). The coastline faces west/north west with a mean high water spring calculated at Bideford of 4.52 m (Halcrow Group, 2010). The region is exposed to high energy open ocean swells during winter, with average mean wave heights (Hs) of 1.67 m, mean peak periods (Ts) of 12.1 s and a mean direction of 281 degrees (Table 4) (NNRCMP, 2023). Storm conditions (+2 standard deviations from mean) produce wave heights 2.84 m and wave periods of 14.3 s and higher (NNRCMP, 2023). The dominant westerly wave conditions reach the shore at an oblique angle driving northward longshore sediment transportation (Pethick, 2007).

The combination of the estuary, tidal regime, ocean waves and dune systems creates a dynamic and complex coastal morphology. Pethick (2007) suggests the presence of an anti-clockwise tidal gyre system in Bideford Bay where sand is moved northward, assisted by longshore wave transport, from Northam beach bypassing the estuary channel onto Saunton where it transported offshore towards Baggy Point and then southwards to Westward Ho! and onto Northam beach. Net accretion of sediments on Saunton has been observed on the southern section (Halcrow Group, 2010; Pethick, 2007). Pethick (2007), estimates that 20 000 m^3 of sediment is being transported and deposited into the estuary per year resulting in a net loss of sediments from the open coast system. The complex sedimentary transportation system at play, data availability and lack of statistical evidence of the anti-clockwise single tidal gyre makes Bideford Bay a suitable site for evaluating PyShoreVolume's ability to provide insights into erosion and accretion rates and driving forces of changes across a coastal system.

4.2. Study Site Data

Lidar data from 9 different dates between 2007 - 2020 was obtained from the National Network of Regional Coastal Monitoring Programmes website (NNRCMP) (Table 5) (Plymouth Coastal Observatory, 2022). Previous reviews of the study site revealed the most mobile section of shoreline was on the southern section of Saunton where a seaward procession was observed (Pethick, 2007). This movement suggests the accretion of sediments deposited from either the inner estuary or from Northam. No NNRCMP data was available since 2020 for this section of shoreline so a terrestrial Lidar survey was performed to assess recent volumetric and shoreline changes. A Riegl VZ-2000i was used to collect topographic data, with scans taking place across 1400 m of shore at 15 m spacings at different cross shore positions to maximise coverage of sand bank contours. The initial point cloud data was processed in RiSCAN Pro removing outliers and exported into a pointcloud '.las' file before conversion into a 1 m pixel resolution GeoTiff DEM using the Points2Grid tool (Kim et al., 2006; RIEGL Laser Management Systems, 2023a,b). Elevation resolutions are 0.001 m throughout the series, with a maximum vertical accuracy variation of +-0.4 m (Table 5). This maximum vertical accuracy value will be used as the LOD threshold where DOD values that fall within this range will be omitted from the LOD volume calculations. Each of the Lidar datasets were processed into DEMs and merged following the protocols set out by Pollard et al. (2019). Baselines were drawn off-shore with transects drawn every 20 m. Shoreline elevation contours at the Mean High Water Spring (MHWS) value were extracted across each of the DEMs using the additional PyQGIS scripts provided. The intersections were created following the PyShoreVolume 'README' documentation. The SCA analysis at Saunton focused on the region of coastline where the 2022 terrestrial surveys were undertaken, which encompass the greatest variations in shoreline position seen in prior analysis.

Table 5
Time Series of Coastal Data Used (NNRCMP, 2021).

Data	Date	Depth Resolution	Vertical Accuracy
Airborne Lidar	03/02/2007	0.001 m	+- 40cm
	09/04/2008	0.001 m	+- 40cm
	09/04/2009	0.001 m	+- 15cm
	04/09/2009	0.001 m	+- 15cm
	06/05/2012	0.001 m	+- ?*cm
	01/04/2014	0.001 m	+- 10cm
	23/02/2016	0.001 m	+- 10cm
	13/02/2017	0.001 m	+- 40cm
	18/09/2020	0.001 m	+- 30cm
Terrestrial Lidar	22/09/2022	0.001 m	+- 5cm

? indicates information not available.

4.3. Results

4.3.1. Shoreline Change Analysis

The SCA outputs at Saunton show the majority of movement is observed on the southern region. The NSM (Figure 5) analysis shows a maximum change of 80.93 m on transect 77 and the NSMEandA (Figure 6) shows the the shoreline is prograding over the majority of this section. Erosion trends on the southern most transects in the figure (transects 104-110) are observed. Maximum retreat of 17.52 m of retreat can be seen at transect 110. The SCE (Figure 7) show the largest rates of change occurred between 09/04/2009 - 13/02/2017 reaching 138.85 m on transect 33. The transects between 63 and 75 show the largest rates across the shoreline each recording 130 m of shoreline movement. The EPR (Figure 8) analysis shows variable rates with a maximum of 5.17 m of shoreline succession per year at transect 77. Transect 104 shows the maximum erosion EPR rate of -1.28 m per year.

On Northam the northern section of the shoreline saw the most erosion (transect 27 - 115), with the highest erosion rate of 51.4 m being observed on transect 50. NSM (Figure 9) and NSMEandA (Figure 10) outputs show that the region between transects 40-63 has experienced over 50 m of erosion between 2007 - 2020. The southern section of the beach which is backed by the pebble ridge shows zones of minor (<5 m) accretion in middle section (transect 117 - 144) and erosion in the southern most transects. The maximum distances reported by SCE (Figure 11) of 61.4 m occurred at transect 58 between 2007-2014. Overall, the envelope changes and EPR calculations (Figure 12) are very similar to erosion and accretion trends, confirming the zone (transects 40 – 63) to be most susceptible to positional change.

4.3.2. Volumetric Change Analysis

The DOD outputs align well with the SCA functions. Figure 13 show the series of DOD plots calculated from the time series of DEMs available at Saunton Sands. The package's function to crop DEMs to the smaller of two in the calculation before computing change within the region of shared data availability (Section 2.3) is demonstrated in Figure 13g. Variable accretion and erosion trends are observed in Figure 13, with plots a, e, f, g showing erosion

across the northern section of beach. Large volumes of accretion (+2 m) can be seen on the southern section of the bay which is closest to Northam Beach in six out of nine DODs. This accretion may be viewed as evidence of northward trajectory of sediment transportation from Northam via the Bideford Bar in the estuary mouth. The varying locations of the accretion seen in this section point towards of continuous and substantial bedform movement throughout the time period. At Northam, Figure 14 shows clear evidence of deposition in the southern sections of the beach across six of the eight plots (Figure 14 b, c, d, f, g, h). Areas of erosion in the VCA plots correspond to areas of erosion observed in the SCA function outputs. Up to 8 m elevation differences can be seen in Figure 14 a, d, e and h. The largest accretionary trends can be seen in the northeastern section, located within the estuary mouth. Evidence of +2 m of elevation change is evident in six of the eight DODs (Figure 14 a, b, c, d, g, h). This corresponds to observations at the southern section of Saunton Sands which is exposed to the estuary mouth.

The largest volume of sediment deposition at Saunton Sands +585 515.3 m^3 occurred between 04/09/2009 and 06/05/2012. Six out of the nine time slices show accretion while the first (03/02/2007 - 09/04/2008), fifth (06/05/2012 - 06/04/2014) and eighth (13/02/2017 - 18/09/2020) DODs produce evidence of considerably high erosion at -567 871.2 m^3, -428 963.2 m^3 and -206 586.4 m^3 respectively. At Northam, the largest volumes of change were observed within the first DOD (03/02/2007-09/04/2008 -223 527.8 m^3) across the 14 month period. The largest amounts of accretion was detected in the seventh DOD (23/02/2016-13/02/2017 +172 656.4 m^3).

When assessing the net volume changes it was decided that the last DEM at Saunton (22/09/2022) would be omitted as it is limited to a region that is known to show net accretion and not areas that may show erosion. Including it may produce skewed results, biased toward showing accretion rates. Using the DEM from 22/09/2020 provides a greater understanding of the changes seen across the system as a whole. The Net Volumetric changes showed a minor increase of sediment volume on Saunton (+59 977.7 m^3), as opposed to Northam where substantial reduction in volumes (-248 116.6 m^3) is observed. The limited volumetric gain at Saunton and substantial loss at Northam suggests a net loss of sediments within the Taw and Torridge coast and estuary system. This equates to an annual sediment gain at Saunton of +4613.6 m^3/year, whilst Northam suffers from a loss of -21 393.6 m^3/year.

A time series of the key oceanographic variables are plotted with the DOD results on Saunton and Northam in Figure 15. A two to four year seasonal trend of erosion and accretion events can be seen across the time series. The erosion events seen on Northam and Saunton in 2014 are found after a winter which recorded over 642 hours of wave height conditions 472 hours of wave period conditions above the 0.95 quantile (+2.34m and +14.3 s), the second and first highest across the period, respectively. This event is followed by a gradual increase in sediment during the following 3 years peaking with the substantial gains observed in 2017. The DODs with the largest volumetric gains (04/09/2009-06/05/2012, 23/02/2016-13/02/2017) are found after winters with lower periods of +0.95 quantile wave height conditions at 281 hours and 171 hours respectively. The packages seasonality functions show no distinct trend in accretion and erosion rates as a result of seasonal climatological and oceanographic changes, though the lack of repeated surveys during specific months mitigate this finding. Overall each of the seasonal functions show net accretion, with only two of the DODs (03/02/2007-23/02/2016, 06/05/2012-01/04/2014) showing erosion between dates.

4.3.3. Discussion and Performance Evaluation

The results of the SCA on the northern section of Northam suggest susceptibility to erosion events with EPR rates suggesting a retreat rate of -3.84 m per year, a trend that if continued will cause inundation of the golf course. However, the pebble ridge which acts as the MHWS interface only shows minor positional movements and stability as whole, with some minor shoreward realignment observed across the southern region, supporting the work of Pethick (2007). The accretion of sediments on the southern section of Saunton found in Figure 13 and the shoreline progradation found

Table 6
Volumetric Change Results from Northam and Saunton Sands

Dates	Season	Volume Changes Saunton (m^3)	Volume Changes Northam (m^3)
03/02/2007 - 09/04/2008	-	-567871.2	-223527.8
09/04/2008 - 09/04/2009	-	+134494.3	+48520.1
09/04/2009 - 04/09/2009	-	+4649.8	-42392.6
04/09/2009 - 06/05/2012	-	+585515.3	+57274.6
06/05/2012 - 01/04/2014	-	–428963.2	-178568.7
01/04/2014 - 23/02/2016	-	+39263.8	-38108.4
23/02/2016 - 13/02/2017	-	+477597.2	+172656.4
13/02/2017 - 18/09/2020	-	-206586.4	-97535.1
19/09/2020 - 22/09/2022	-	+51846.5	N/D
03/02/2007 - 23/02/2016	Winter	-228275.3	-363020.3
23/02/2016 - 13/02/2017	Winter	+477597.2	+172656.4
09/04/2008 - 09/04/2009	Spring	+134494.3	+48520.1
09/04/2009 - 06/05/2012	Spring	+588238.8	+14219.1
06/05/2012 - 01/04/2014	Spring	-428963.2	-178568.9
04/09/2009 - 18/09/2020	Autumn	+491516.8	-59645
18/09/2020 - 22/09/2022	Autumn	+51846.6	N/D*
Net Change (03/02/2007 - 04/09/2020)	-	+59977.7	-278116.6
Net Change LOD (03/02/2007 - 18/09/2020)	-	+262201.8	-247380.5

*N/D indicates No Data.

in the SCA plots of Saunton suggest sediment deposition from Northam as identified by Pethick (2007). The dominant south westerly wave directions (Figure 15) cause waves to arrive on the shoreline at an oblique angle, and are believed to drive longshore transportation of finer sediments from Northam (Dubois, 1988; Short, 2012). Seasonal volumetric change statistics point to an accretion trends in the Autumn, however the sparse amount of repeated surveys at similar times of year limit the ability to draw conclusive results on the effects of climatic seasonality.

Evidence of the Bideford Bay single gyre, proposed by Pethick (2007) is observed, with a trend of deposition identified on the southern region of Northam, while conversely the northern section of Saunton shows susceptibility to erosion. The two to three year erosion and deposition trends observed across the time series in Figure 15 give further support for tidal re-circulatory system. Erosion events driven by high intensity storm events such as those observed in the winter of 2013/14 (Figure 15) are believed to remove sediment from the beaches, offshore into the sub-aqueous gyre system. The lack of an obvious sediment source and the continued re-supply of sediment to the bay suggest the sediments are kept within the bay gyre and are transported in an anti-clockwise direction. From here the sediments are

steadily re-deposited across the bay with more concentrated volumes found on the southern part of Northam. The trend of re-deposition is observed over a 2-4 year period and may be assisted by periods of limited intensity winter storm seasons (Pethick, 2007). It is currently unknown whether the volumetric losses occur over a single event or due to prolonged periods of wave and storm intensity. Up until now, no study has observed this multi-year trend or identified a time-frame for the erosion and deposition events seen across this system.

The net volume changes and changes observed when integrating the LOD error in the calculations across the whole period provide somewhat contradictory results. The net volume change statistics support the findings of Pethick (2007) that a sediment loss of -20 000m^3/year from the open coast system through deposition within the Taw and Torridge Estuary is occurring with a combined volume loss of -16 779 m^3/year being observed across the shorelines. However, LOD results show sediment losses from Northam (-19 029.3 m^3/year) are approximately equal to volumetric gains at Saunton (+20 169.4 m^3/year). On this basis then deposition within the estuary can be viewed as negligible, suggesting there is limited sediment loss to the inner estuary and that the single gyre system is a weaker driver of sediment deposition than the erosional ocean-dominated long shore transportation drivers. This emphasises the need for further work assessing the drivers of volumetric changes within the Taw and Torridge estuary. In either case, the evidence shows that Northam has a sediment budget imbalance which could be a contributing factor to the shoreline erosion observed on the northern sections of Northam beach, as sediment loss and ensuing shoreline height changes, may allow high energy destructive waves to reach and erode the MHWS shoreline contour (Enríquez et al., 2016; Griggs and Reguero, 2021; Tavares et al., 2020).

The application of PyShoreVolume at the Taw and Torridge Estuary confirms it is computationally efficient, produces a series of useful graphical outputs from which shoreline and volumetric changes can be readily visualised and interpreted, with no GIS-based map production needed due to the utilisation of geospatial libraries. The production of statistics from each method in the form of a Pandas DataFrame also allows further mathematical and statistical analysis to be quickly and easily performed. The package enabled in depth analysis of the Taw and Torridge Estuary open coast system, producing shoreline change rates, identifying vulnerable locations and providing supportive evidence to the predicted volumetric losses identified by Pethick (2007). It has also provided a means by which to understand the time-frame of erosion and recharge rates of the tidal gyre system proposed by Pethick (2007).

4.3.4. Limitations

Though effective, PyShoreVolume has some limitations that are priorities for future development. The transect creation process in QGIS does not yet allow individual transect azimuths to be set which can lead to cross over of transects when projected on a curved offshore baseline. Further work could focus on creating Python functions that can automatically create an offshore baseline, draw transects that do not cross over when projected from a non-linear

base and can create and save the intersection shapefile used for the analysis functions. Ultimately this would remove the need any work within QGIS, allowing a workflow based solely within Python, which would further reduce processing time. Furthermore, PyShoreVolume has no Weighted Linear Regression Rate (WLRR) function which is present within the AMBUR and DSAS systems. This metric is a variation of LLR where shorelines with minimum error ranges are given greater weight when determining the linear best fit line, which can help alleviate the influence of shorelines extracted from older data sets with larger error ranges (Himmelstoss et al., 2021). WLRR was not included in this version as it would be redundant when using the recent, high resolution and accurate data from the NNRCMP. The toolkit also does not contain forecasting functions as available in DSAS and EPR4Q (De Lima et al., 2021; Himmelstoss et al., 2021). It may also be noted that the SCE, NSM and NSMEandA functions do not provide horizontal error into the measurements, however, we feel that the ability to integrate error into the EPR function and the linear regression statistics such as standard error, R-squared and P-value produced in the LRR function goes some way to mitigate this limitation. Future releases may include forecasting operations that utilise EPR calculations to help predict shoreline positions to a defined period of time and provide an ability to include horizontal error in the SCE, NSM and NSMEandA functions.

In regards to VCA, future work should focus on segmentation techniques that allow improved sediment transportation tracking. Each of these methods were used to effect by Burvingt et al. (2017) allowing better classification of beaches in response to climatological events. At present each DEM in the time series needs to have the same spatial resolution per pixel for the DOD functions to produce accurate graphics and volumetric results. Control systems could be added to the Masking function that automates a shared spatial resolution between DEMs so analytical VCA functions can operate correctly.

5. Conclusions

The PyShoreVolume package aims to provide an open source Python based tool that can perform a range of Shoreline Change and Volumetric Change analysis functions after limited amounts of pre-processing, thus, allowing rapid reproducible assessments of the coastal zone. The performance of the SCA functions were tested against already well established open source (AMBUR) and licenced (DSAS) systems using the same data sets and produced near perfect correlations. Package documentation allows users to easily create the two necessary geospatial data files (Transects, Intersections) needed to use PyShoreVolume SCA functions. The package has functions to combine, clean and add errors ranges to the datasets, proved to be efficient and produces a range of easily interpretable graphics that identify rates of change and at risk regions of the shoreline. The package reduces the users need to use mapping tools to plot the areas under assessment, and allows users to further assess the results within a Python IDE in the form of a Pandas DataFrame. The volumetric functions allow automated spatial assessments of the height changes and

volumetric changes across the study region. These functions use Digital Elevation Model of Difference calculations, permitting areas of erosion and accretion to be easily identified in graphical outputs and overall volumetric changes to be calculated, which can be used to interpret the drivers of morphological change. The package's seasonality functions can help identify impacts of seasonal climatic and oceanographic conditions such as wave power.

The functional ability of PyShoreVolume to perform SCA and VCA was shown through a case study of the Taw and Torridge Open Coast and Estuary system. Using data provided by the Plymouth Coastal Observatory each function was performed, providing graphics and statistics that went some way to providing evidence for the single gyre conceptual model put forward by Pethick (2007). Contradictory results for Net Volume and Net Volume Limit of Detection functions suggest further work needs to be made to better understand the sediment transportation processes at the site. It is thought that the losses seen on Northam may be a contributing factor to the high levels of erosion seen on the northern section of beach.

6. Acknowledgments

The authors would like to acknowledge Plymouth Coastal Observatory and the National Network of Regional Coastal Monitoring Programmes for providing the open sourced data used in this study. This work was funded through a studentship awarded to Owen Casey James via the London NERC Doctoral Training Partnership (NE/S007229/1).

PyShoreVolume 1.0.0

Code availability section

PyShoreVolume 1.0.0

Contact: owen.james@kcl.ac.uk

Developers: Owen Casey James.

Program language: Python 3+

Software required: QGIS 3 LTR (3.2+), Python 3.

Program size: 1.3 MB

The source codes are available for downloading at the link: https://pypi.org/project/PyShoreVolume/

Or on the Git-Hub repository: https://github.com/owencaseyjames/PyShoreVolume.git

References

Aagaard, T., Davidson-Arnott, R., Greenwood, B., Nielsen, J., 2004. Sediment supply from shoreface to dunes: linking sediment transport measurements and long-term morphological evolution. Geomorphology 60, 205–224. doi:10.1016/J.GEOMORPH.2003.08.002.

Arrabas-Bel, D., 2020. Introduction guide to contextily — contextily 1.1.0 documentation. URL: https://contextily.readthedocs.io/en/latest/intro_guide.html.

Balaji, R., Kumar, S.S., Misra, A., 2017. Understanding the effects of seawall construction using a combination of analytical modelling and remote sensing techniques: Case study of Fansa, Gujarat, India. https://doi.org/10.1177/1759313117712180 8, 153–160. URL: https://journals.sagepub.com/doi/10.1177/1759313117712180, doi:10.1177/1759313117712180.

Bloom, T.D., Flower, A., DeChaine, E.G., 2018. Why georeferencing matters: Introducing a practical protocol to prepare species occurrence records for spatial analysis. Ecology and Evolution 8, 765–777. URL: https://onlinelibrary.wiley.com/doi/full/10.1002/ece3.3516https://onlinelibrary.wiley.com/doi/abs/10.1002/ece3.3516https://onlinelibrary.wiley.com/doi/10.1002/ece3.3516, doi:10.1002/ECE3.3516.

Burningham, H., Fernandez-Nunez, M., 2020. Shoreline change analysis. Sandy Beach Morphodynamics , 439–460doi:10.1016/B978-0-08-102927-5.00019-9.

Burningham, H., French, J., 2017. Understanding coastal change using shoreline trend analysis supported by cluster-based segmentation. Geomorphology 282, 131–149. doi:10.1016/J.GEOMORPH.2016.12.029.

Burvingt, O., Masselink, G., Russell, P., Scott, T., 2017. Classification of beach response to extreme storms. Geomorphology 295, 722–737. doi:10.1016/J.GEOMORPH.2017.07.022.

Carvalho, R.C., Allan, B., Kennedy, D.M., Leach, C., O'Brien, S., Ierodiaconou, D., 2021. Quantifying decadal volumetric changes along sandy beaches using improved historical aerial photographic models and contemporary data. Earth Surface Processes and Landforms 46, 1882–1897. doi:10.1002/ESP.5130.

De Lima, L.T., Fernández-Fernández, S., Espinoza, J.M.D.A., Albuquerque, M.D.G., Bernardes, C., 2021. End Point Rate Tool for QGIS (EPR4Q): Validation Using DSAS and AMBUR. ISPRS International Journal of Geo-Information 2021, Vol. 10, Page 162 10, 162. URL: https://www.mdpi.com/2220-9964/10/3/162/htmhttps://www.mdpi.com/2220-9964/10/3/162, doi:10.3390/IJGI10030162.

Dubois, R.N., 1988. Seasonal changes in beach topography and beach volume in Delaware. Marine Geology 81, 79–96. doi:10.1016/0025-3227(88)90019-9.

Enríquez, A.R., Marcos, M., Álvarez-Ellacuría, A., Orfila, A., Gomis, D., 2016. Changes in beach shoreline due to sea level rise and waves under climate change scenarios: application to the Balearic Islands (Western Mediterranean) doi:10.5194/nhess-2016-361.

Esmukov, K., 2022. GeoPy Documentation Release 2.3.0. URL: https://buildmedia.readthedocs.org/media/pdf/geopy/latest/geopy.pdf.

Gares, P.A., Wang, Y., White, S.A., 2006. Using LIDAR to Monitor a Beach Nourishment Project at Wrightsville Beach, North Carolina, USA. https://doi.org/10.2112/06A-0003.1 2006, 1206–1219. URL: https://bioone.org/journals/journal-of-coastal-research/volume-2006/issue-225/06A-0003.1/Using-LIDAR-to-Monitor-a-Beach-Nourishment-Project-at-Wrightsville/10.2112/06A-0003.1.fullhttps://bioone.org/journals/journal-of-coastal-research/volume-2006/issue-225/06A-0003.1/Using-LIDAR-to-Monitor-a-Beach-Nourishment-Project-at-Wrightsville/10.2112/06A-0003.1.short, doi:10.2112/06A-0003.1.

Gillies, S., 2023. rasterio Documentation Release 1.4dev. URL: https://rasterio.readthedocs.io/_/downloads/en/latest/pdf/.

Google, 2023. Bideford Bay, North Devon, England. URL: https://mt1.google.com/vt/lyrs=s&x={x}&y={y}&z={z}.

Griggs, G., Reguero, B.G., 2021. Coastal Adaptation to Climate Change and Sea-Level Rise. Water 2021, Vol. 13, Page 2151 13, 2151. URL: https://www.mdpi.com/2073-4441/13/16/2151/htmhttps://www.mdpi.com/2073-4441/13/16/2151, doi:10.3390/W13162151.

Grilli, S.T., Horrillo, J., 1970. Short-term Shoreline Change On the Sendai Coast. WIT Transactions on The Built Environment 10, 8. URL: http://www.witpress.com/elibrary/wit-transactions-on-the-built-environment/10/10010, doi:10.2495/CE950231.

Hackeloeer, A., Klasing, K., Krisp, J.M., Meng, L., 2014. Georeferencing: a review of methods and applications. https://doi.org/10.1080/19475683.2013.868826 20, 61–69. URL: https://www.tandfonline.com/doi/abs/10.1080/19475683.2013.868826, doi:10.1080/19475683.2013.868826.

Halcrow Group, 2010. North Devon and Somerset Shoreline Management Plan. Technical Report. URL: https://southwest.coastalmonitoring.org/wp-content/uploads/NDASCAG_SMP2/Appendices/Appendix_C_Baseline_Processes.pdf.

Himmelstoss, E.A., Henderson, R.E., Kratzmann, M.G., Farris, A.S., 2021. Digital Shoreline Analysis System (DSAS) Version 5.1 User Guide Open-File Report 2021-1091 .

Jackson, C.W., Alexander, C.R., Bush, D.M., 2012. Application of the AMBUR R package for spatio-temporal analysis of shoreline change: Jekyll Island, Georgia, USA. Computers and Geosciences 41, 199–207. URL: www.elsevier.com/locate/cageo, doi:10.1016/j.cageo.2011.08.009.

Jackson, D.W., Cooper, J.A., Del Rio, L., 2005. Geological control of beach morphodynamic state. Marine Geology 216, 297–314. doi:10.1016/J.MARGEO.2005.02.021.

Jackson, D.W.T., Short, A.D., 2020. Introduction to beach morphodynamics. Sandy Beach Morphodynamics , 1–14doi:10.1016/B978-0-08-102927-5.00001-1.

Jordahl, K., Van den Bossche, J., Fleischmann, M., Wasserman, J., McBride, J., Gerard, J., Tratner, J., Perry, M., Garcia Badaracco, A., Farmer, C., Arne Hjelle, G., Snow, A.D., Cochran, M., Gillies, S., Culberston, L., Bartos, M., Eubank, N., Albert, M., Bilogur, A., Rey, S., Ren, C., Arribas-Bel, D., Wasser, L., Wolf, L.J., Journois, M., Wilson, J., Greenhall, A., Holdgraf, C., Filipe, Leblanc, F., 2020. GeoPandas 0.13.0 Documentation. URL: https://geopandas.org/en/stable/about/citing.html.

Kim, H., Arrowsmith, J., Crosby, C.J., Jaeger-Frank, E., Nandigam, V., Memon, A., Conner, J., Baden, S.B., Baru, C., Kim, H., Arrowsmith, J., Crosby, C.J., Jaeger-Frank, E., Nandigam, V., Memon, A., Conner, J., Baden, S.B., Baru, C., 2006. An Efficient Implementation of a Local Binning Algorithm for Digital Elevation Model Generation of LiDAR/ALSM Dataset. AGUFM 2006, G53C–0921. URL: https://ui.adsabs.harvard.edu/abs/2006AGUFM.G53C0921K/abstract.

Kim, H.G., Meissner, C., 2017. Correction of LiDAR measurement error in complex terrain by CFD on JSTOR. URL: https://www.jstor.org/stable/90011109.

Leafe, R., Pethick, J., Townend, I., 1998. Realizing the Benefits of Shoreline Management. The Geographical Journal 164, 282. doi:10.2307/3060617.

Luijendijk, A., Hagenaars, G., Ranasinghe, R., Baart, F., Donchyts, G., Aarninkhof, S., 2018. The State of the World's Beaches. Scientific Reports 2018 8:1 8, 1–11. URL: https://www.nature.com/articles/s41598-018-24630-6, doi:10.1038/s41598-018-24630-6.

Morton, R.A., 1975. G TEXAS BUR. OF "TC ft AN ANALYSIS OF HISTORICAL CHANGES OF THE TEXAS GULF SHORELINE The Texas Gulf Shoreline. Geological Circular 75.

NNRCMP, 2021. National Coastal Monitoring - Welcome. URL: https://coastalmonitoring.org/.

NNRCMP, 2022. National Coastal Monitoring - Welcome. URL: https://coastalmonitoring.org/.

NNRCMP, 2023. Bideford Bay Wave Buoy Summary Statistics. URL: https://coastalmonitoring.org/realtimedata/?chart=97&tab=stats&disp_option=&data_type=table&year=All%20years.

Pandas development team, 2023. pandas-dev/pandas: Pandas. URL: https://doi.org/10.5281/zenodo.3509134, doi:10.5281/ZENODO.7857418.

Paola, G.D., Rodríguez, G., Rosskopf, C.M., 2023. Shoreline Dynamics and Beach Erosion. Geosciences 2023, Vol. 13, Page 74 13, 74. URL: https://www.mdpi.com/2076-3263/13/3/74/htmhttps://www.mdpi.com/2076-3263/13/3/74, doi:10.3390/GEOSCIENCES13030074.

Pethick, J., 2007. The Taw-Torridge Estuaries: Geomorphology and Management Report to Taw-Torridge Estuary Officers Group URL: https://www.northdevonbiosphere.org.uk/uploads/1/5/4/4/15448192/taw_torridge_and_approaches_coastal_evolution_study.pdf.

Plymouth Coastal Observatory, 2022. Home - SWRCMP. URL: https://southwest.coastalmonitoring.org/.

Pollard, J.A., Brooks, S.M., Spencer, T., 2019. Harmonising topographic & remotely sensed datasets, a reference dataset for shoreline and beach change analysis. Scientific Data 2019 6:1 6, 1–14. URL: https://www.nature.com/articles/s41597-019-0044-3, doi:10.1038/s41597-019-0044-3.

Python, 2023. Python 3.11.3 Documentation. URL: https://docs.python.org/3/.

QGIS, 2023. QGIS Documentation Site. URL: https://www.qgis.org/en/docs/index.html.

RIEGL Laser Management Systems, 2023a. RIEGL - Produktdetail. URL: http://www.riegl.com/nc/products/terrestrial-scanning/produktdetail/product/scanner/58/.

RIEGL Laser Management Systems, 2023b. RIEGL - RiSCAN PRO. URL: http://www.riegl.com/products/software-packages/riscan-pro/.

Roy, P., Cowell, P., Ferland, M., Thom, B., 1995. Wave-dominated coasts. Encyclopedia of Earth Sciences Series 14, 121–186. URL: https://www.cambridge.org/core/books/coastal-evolution/wavedominated-coasts/B56E3C051526522DE0FE908740CA19A1, doi:10.1017/CBO9780511564420.006.

Short, A., 2012. Coastal Processes and Beaches | Learn Science at Scitable. URL: https://www.nature.com/scitable/knowledge/library/coastal-processes-and-beaches-26276621/.

Stive, M.J., de Vriend, H.J., 1995. Modelling shoreface profile evolution. Marine Geology 126, 235–248. doi:10.1016/0025-3227(95)00080-I.

Tavares, K.D., Fletcher, C.H., Anderson, T.R., 2020. Risk of shoreline hardening and associated beach loss peaks before mid-century: Oahu, Hawaii. Scientific Reports 2020 10:1 10, 1–10. URL: https://www.nature.com/articles/s41598-020-70577-y, doi:10.1038/

s41598-020-70577-y.

Vos, K., Splinter, K.D., Harley, M.D., Simmons, J.A., Turner, I.L., 2019. CoastSat: A Google Earth Engine-enabled Python toolkit to extract shorelines from publicly available satellite imagery. Environmental Modelling & Software 122, 104528. doi:10.1016/J.ENVSOFT.2019.104528.

Wheaton, J.M., Brasington, J., Darby, S.E., Sear, D.A., 2010. Accounting for uncertainty in DEMs from repeat topographic surveys: Improved sediment budgets. Earth Surface Processes and Landforms 35, 136–156. doi:10.1002/ESP.1886.

List of Figures

PyShoreVolume 1.0.0

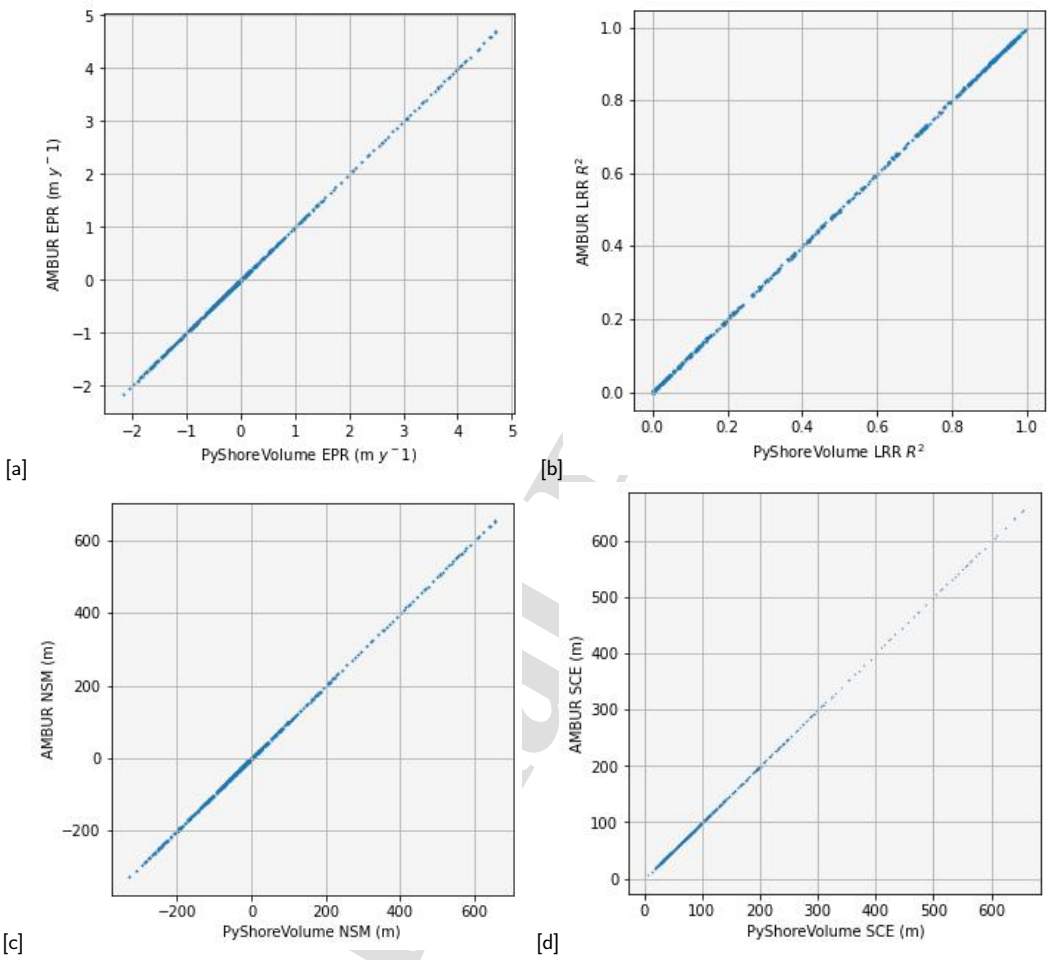

Figure 1: Correlation and T-test analysis of Distance and End Point Rate calculations between AMBUR and PyShoreVolume, each set of results showed Normal Distributions. a) EPR Scatter (Pearsons Correlation R=0.99, P < 0.001, T-Test t < 0.001, p=0.99) b) LRR Scatter Plot (Pearsons Correlation R=0.97, P < 0.001, T-Test t=-0.01, p=0.99) c) NSM Scatter Plot (Pearsons Correlation R=0.99, P < 0.001, T-Test t= < 0.001, p=0.99) d) SCE Scatter Plot (Pearsons Correlation R=0.99, P < 0.001,T-Test t=0.008, p=0.99).

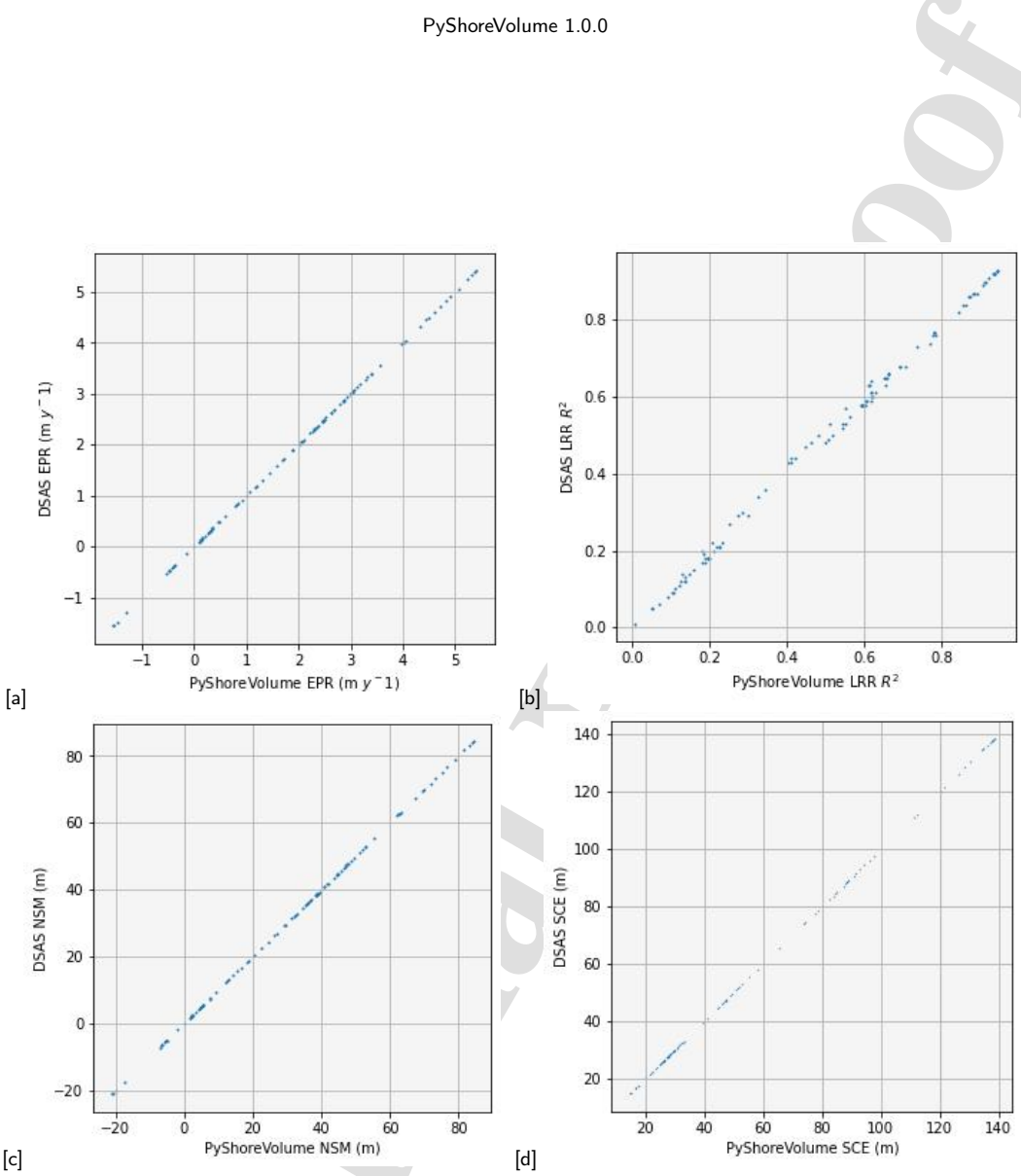

Figure 2: Correlation analysis of Distance and End Point Rate calculations between DSAS and PyShoreVolume, each set of results showed Normal Distributions. a) EPR Scatter (Pearsons Correlation R=0.99, P < 0.001, T-Test t= 0.001, p=0.99) b) LRR Scatter Plot (Pearsons Correlation R=0.99, P < 0.001, T-Test t=-0.17, p=0.86) c) NSM Scatter Plot (Pearsons Correlation R=0.99, P = 0.0, T-Test t=0.001, p=0.99) d) SCE Scatter Plot (Pearsons Correlation R=0.99, P = 0.0,T-Test t < 0.001, p=0.99).

PyShoreVolume 1.0.0

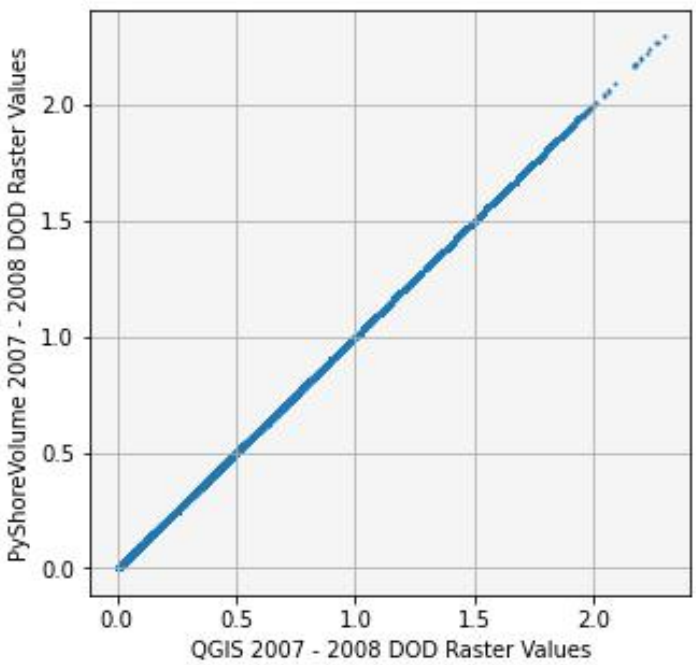

Figure 3: Correlation analysis of Digital Elevation Model of Difference Results from QGIS and PyShoreVolume. Pearsons Correlation Coefficient show identical results between the two systems (R = 1.0, P = 0.0).

PyShoreVolume 1.0.0

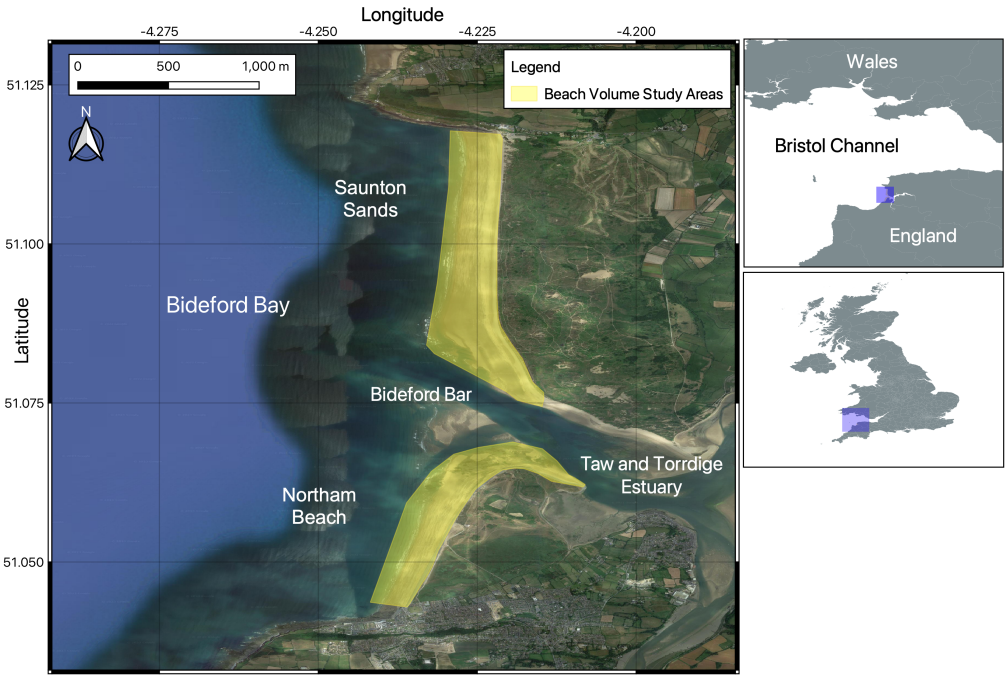

Figure 4: Study site area's Bideford Bay, North Devon, UK. The highlighted areas show the extent to which the DEMs will be cropped to, while the extracted contours at the MHWS mark fall within these boundaries. Map uses OSGB36 / British National Grid EPSG:27700 Coordinate Reference System. (Google, 2023; QGIS, 2023)

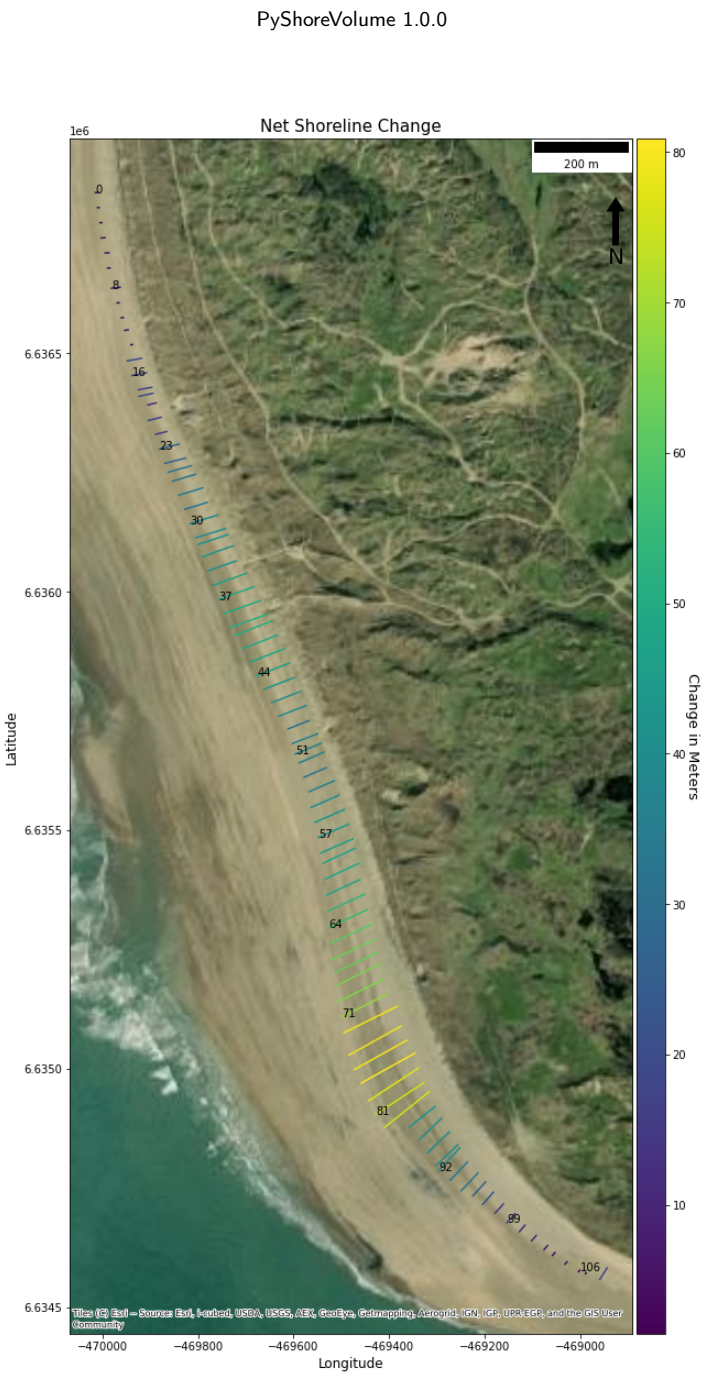

Figure 5: Net Shoreline Movement Output on Saunton Sands, North Devon. Image shows the distance between the oldest and most recent shoreline along each transect. The shoreline change distance of each transect is indicated by a colour gradient shown by the scale bar on the right of the image. Plot coordinates are in WGS 84 / Pseudo-Mercator EPSG:3857.

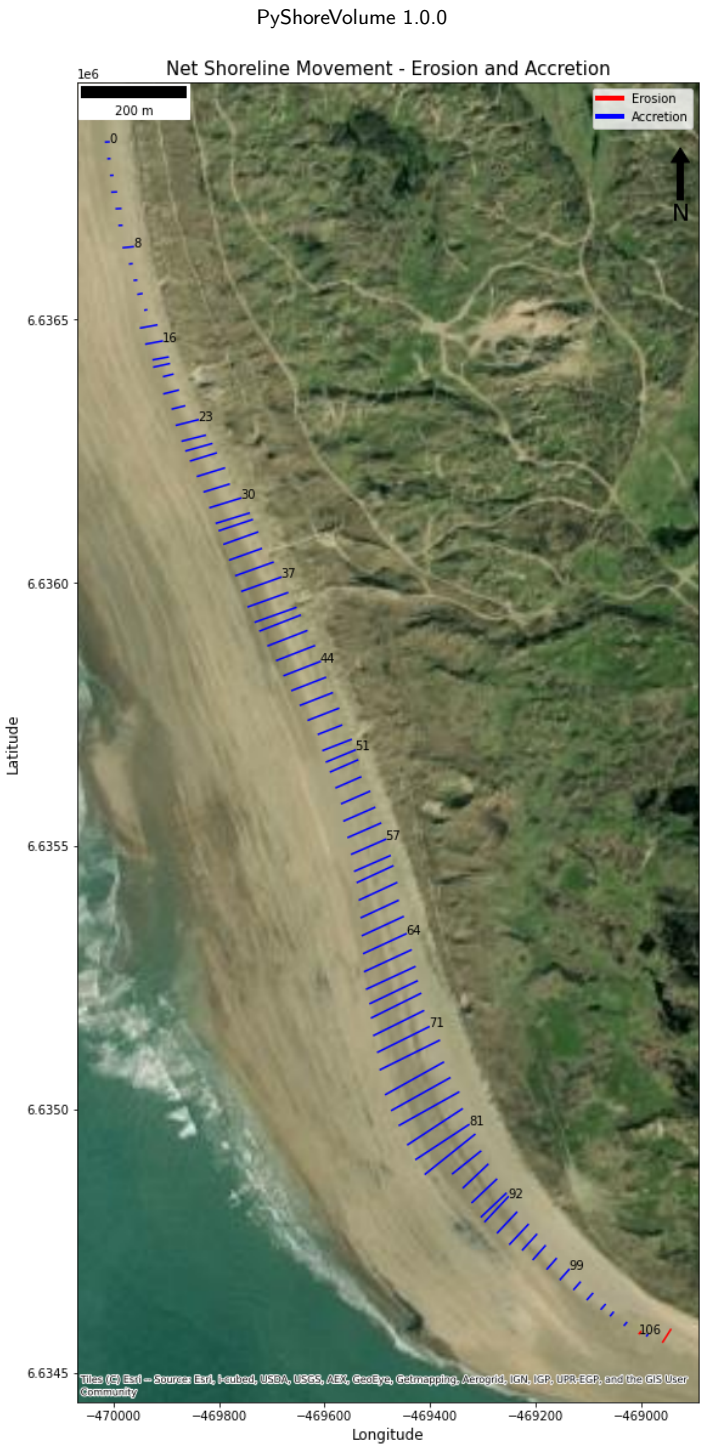

Figure 6: Net Shoreline Movement Erosion and Accretion Output on Saunton Sands, North Devon. Image shows the distance between the oldest and most recent shoreline along each transect. The shoreline change type of each transect is indicated by red (erosion), and blue (accretion). Plot coordinates are in WGS 84 / Pseudo-Mercator EPSG:3857.

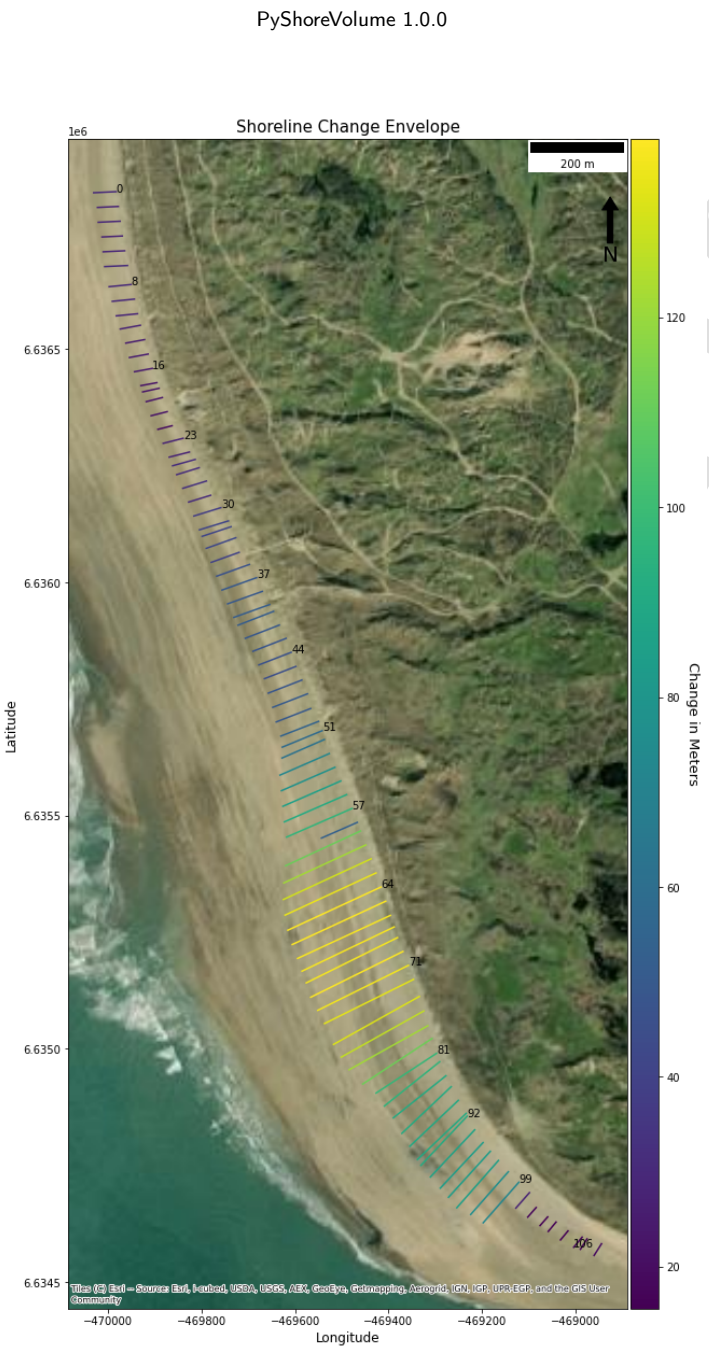

Figure 7: Shoreline Change Envelope Output on Saunton Sands, North Devon. Image shows the maximum shoreline change distance between any of the shorelines present. The shoreline change distance of each transect is indicated by a colour gradient shown by the scale bar on the right of the image. Plot coordinates are in WGS 84 / Pseudo-Mercator EPSG:3857 Coordinate Reference System.

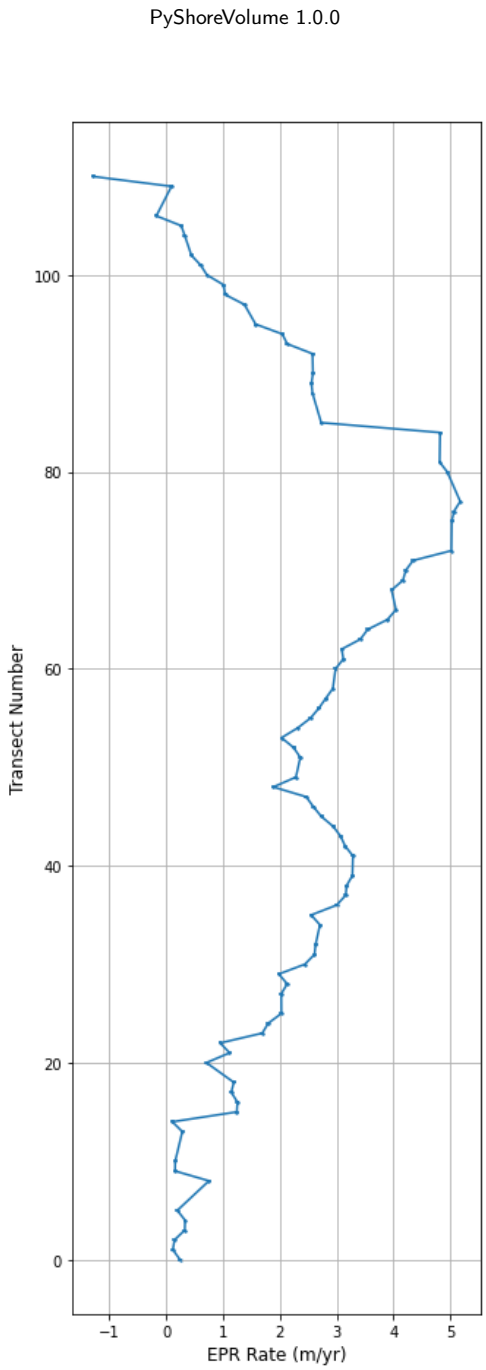

Figure 8: End Point Rate Output on Saunton Sands, North Devon. Indicates the End Point Rate calculated on each transect in meters per year, negative EPR indicates erosion, positive EPR indicates accretion. Error bars are plotted using the 0.4m-+ measurement error ranges from the original Lidar dataset metadata.

PyShoreVolume 1.0.0

Figure 9: Net Shoreline Movement Erosion and Accretion Output Northam Beach, North Devon. Net Shoreline Movement Output on Saunton Sands, North Devon. Image shows the distance between the oldest and most recent shoreline along each transect. The shoreline change distance of each transect is indicated by a colour gradient shown by the scale bar on the right of the image. Plot coordinates are in WGS 84 / Pseudo-Mercator EPSG:3857 Coordinate Reference System.

PyShoreVolume 1.0.0

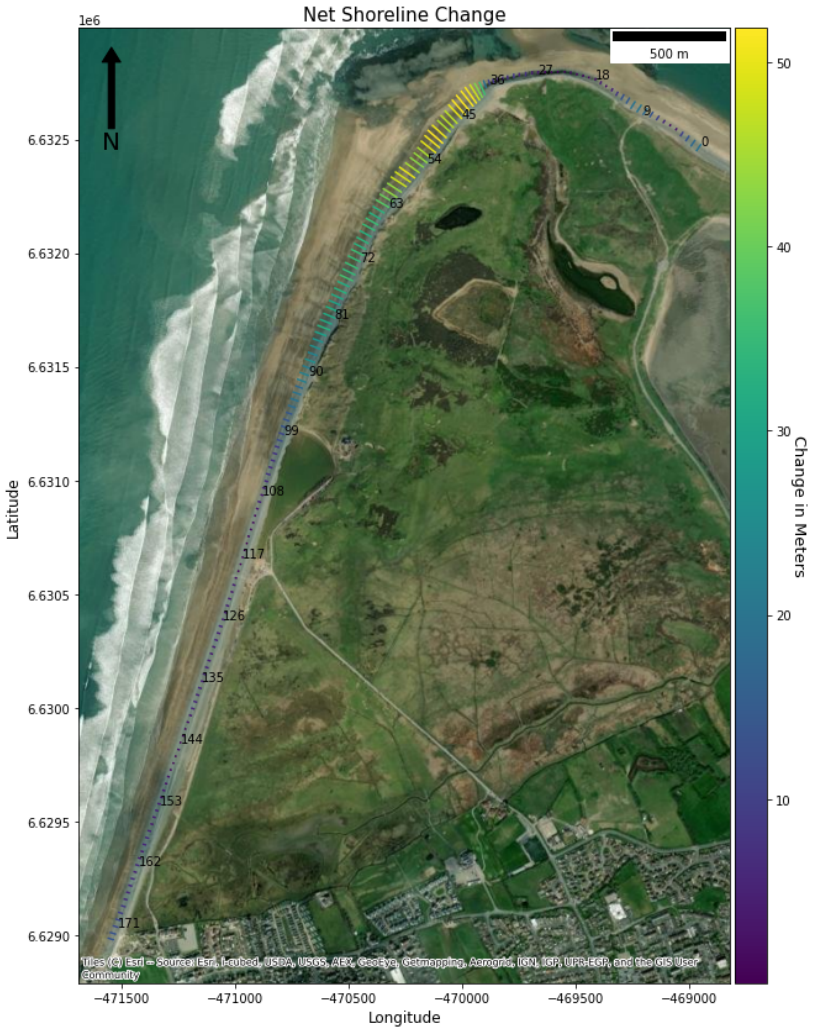

Figure 10: Net Shoreline Movement Output Northam Beach, North Devon. Image shows the distance between the oldest and most recent shoreline along each transect. The shoreline change type of each transect is indicated by red (erosion), and blue (accretion). Plot coordinates are in WGS 84 / Pseudo-Mercator EPSG:3857 Coordinate Reference System.

PyShoreVolume 1.0.0

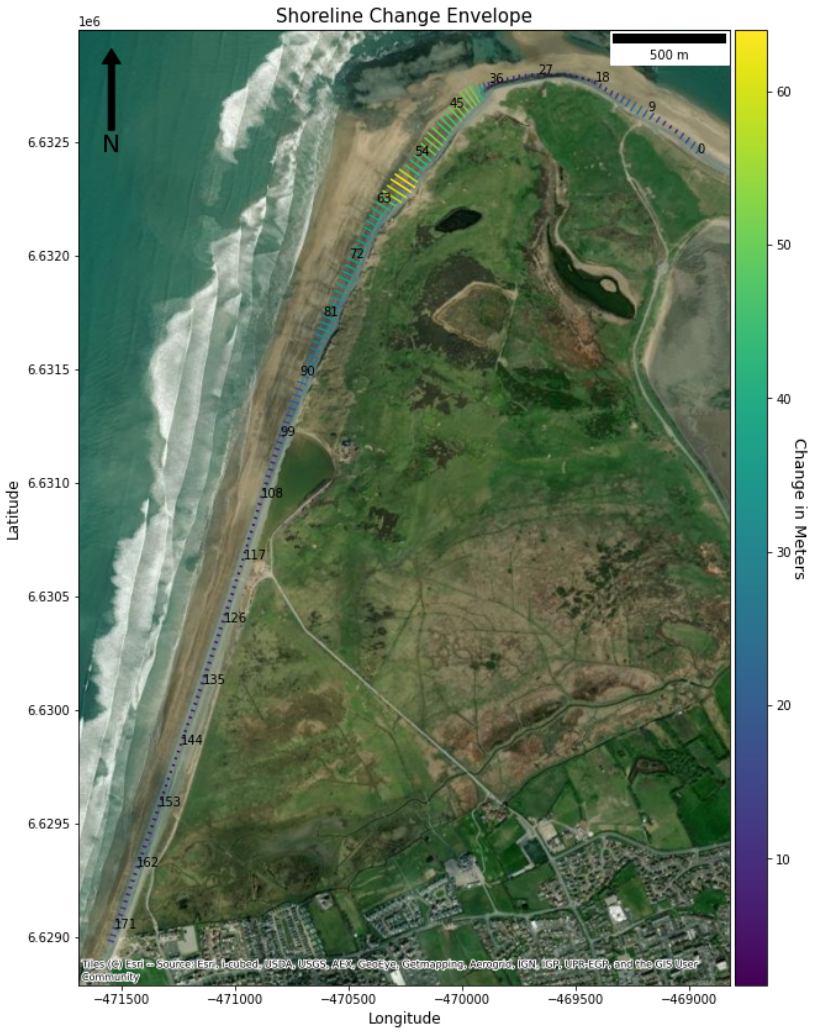

Figure 11: Shoreline Change Envelope Output on Northam Beach, North Devon. Shoreline Change Envelope Output on Saunton Sands, North Devon. Image shows the maximum shoreline change distance between any of the shorelines present. The shoreline change distance of each transect is indicated by a colour gradient shown by the scale bar on the right of the image. Plot coordinates are in WGS 84 / Pseudo-Mercator EPSG:3857 Coordinate Reference System.

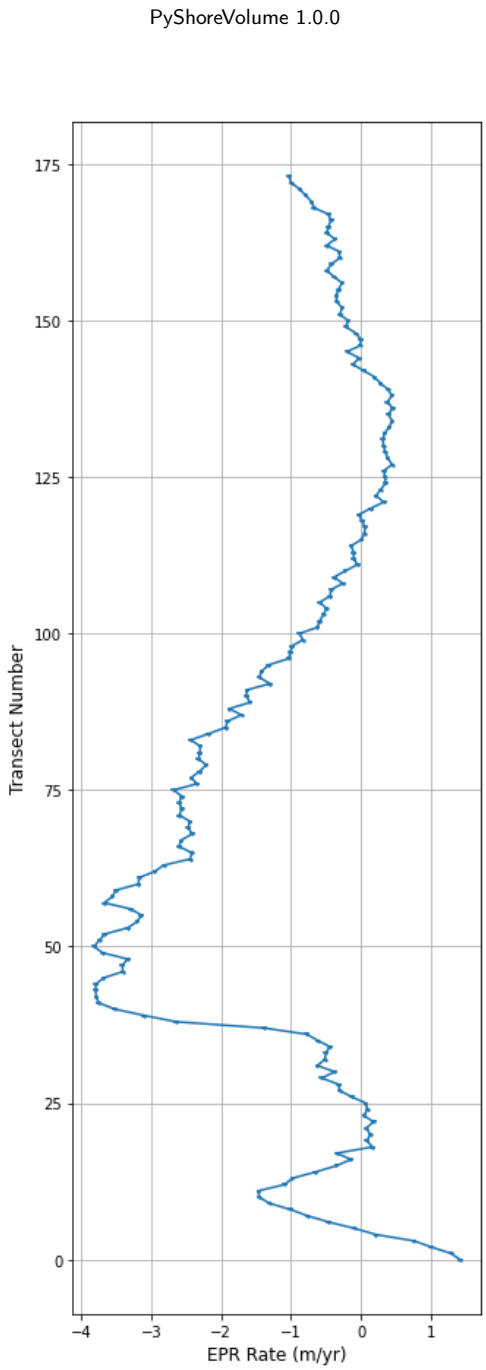

Figure 12: End Point Rate Output on Northam Beach, North Devon. Indicates the End Point Rate calculated on each transect in meters per year, negative EPR indicates erosion, positive EPR indicates accretion. Error bars are plotted using a 0.4m-+ error ranges from the original Lidar dataset metadata.

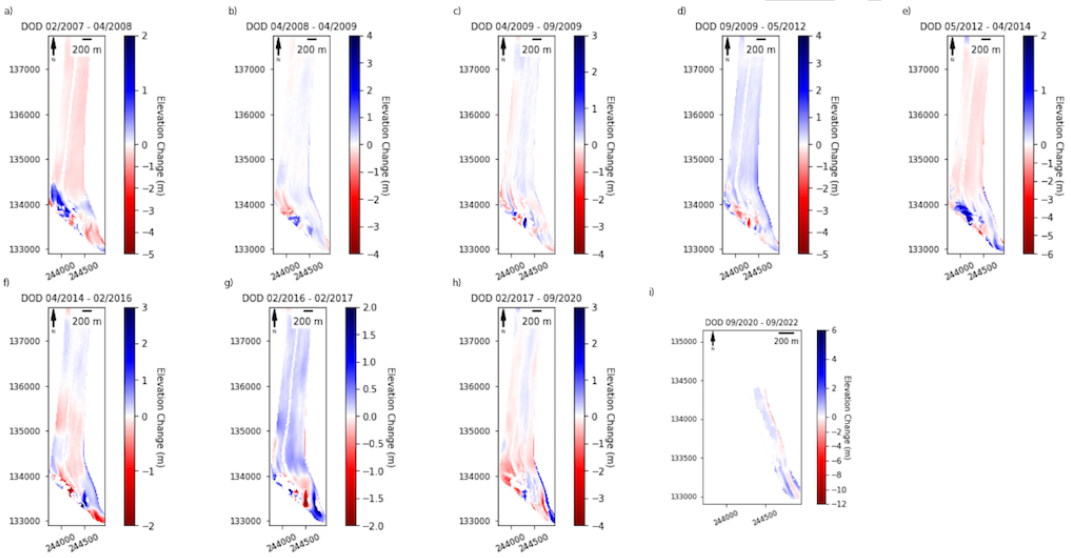

Figure 13: Time Series of Elevation Models of Differences from Saunton Sands, shows erosion (red) and accretion (blue) rates between each consecutive elevation model in the series. From top left to the right (a) 03/02/2007-09/04/2008 (b) 09/04/2008-09/04/2009 (c) 09/04/2009-04/09/2009 (d) 04/09/2009-06/05/2012 (e) 06/05/2012-01/04/2014 (f) 01/04/2014-23/02/2016 (g) 23/02/2016-13/02/2017 (h) 13/02/2017-18/09/2020 (i) 18/09/2020-22/09/2022. Please note the smaller coordinates of the in the final plot. All plots are in OSGB36 / British National Grid EPSG:27700 Coordinate Reference System.

PyShoreVolume 1.0.0

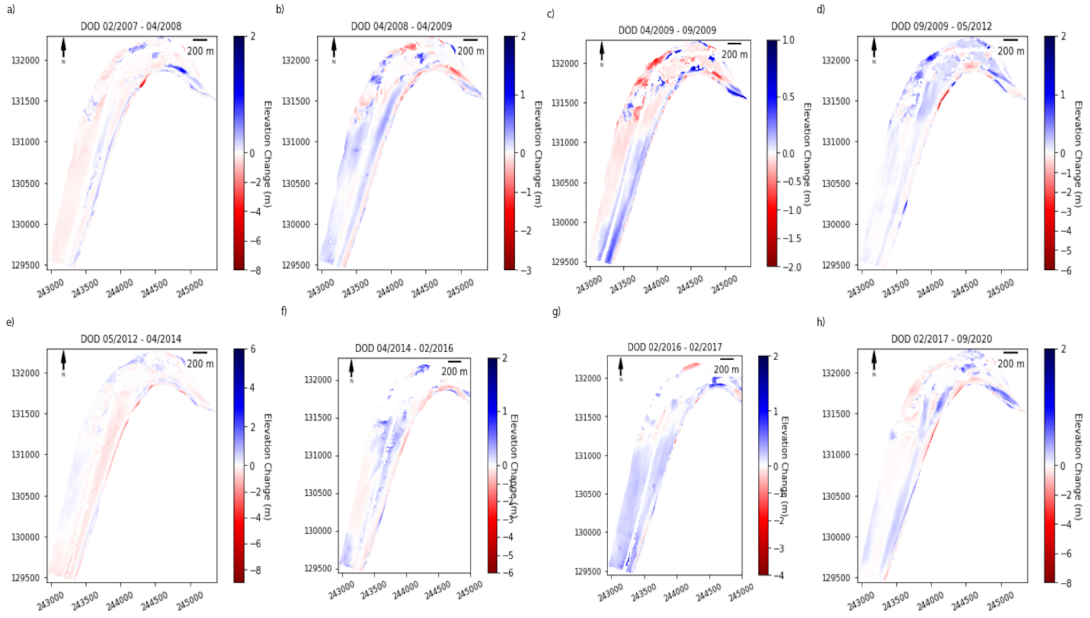

Figure 14: Time Series of Elevation Models of Differences from Northam Burrows, show erosion (red) and accretion (blue) rates between each consecutive elevation model in the series. (a) 03/02/2007-09/04/2008 (b) 09/04/2008-09/04/2009 (c) 09/04/2009-04/09/2009 (d) 04/09/2009-06/05/2012 (e) 06/05/2012-01/04/2014 (f) 01/04/2014-23/02/2016 (g) 23/02/2016-13/02/2017 (h) 13/02/2017-18/09/2020. Please note the smaller coordinates of the in the final plot. All plots have OSGB36 / British National Grid EPSG:27700 Coordinate Reference System.

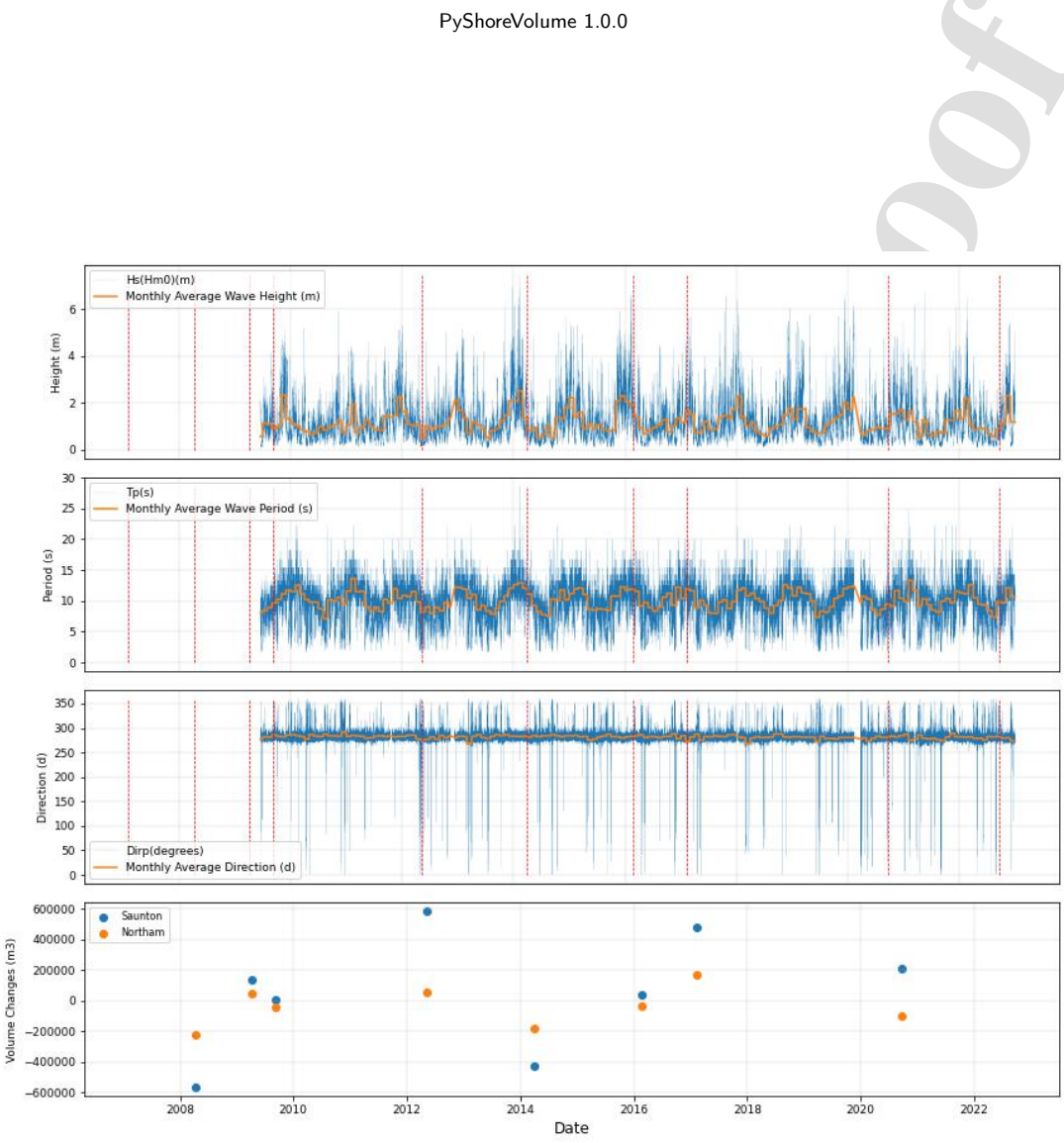

Figure 15: Time Series of Oceanographic Parameters and Volumetric Changes at Saunton and Northam. From the top - First: Hourly significant wave height (blue) and monthly average wave height (orange). Second: Hourly wave period (blue) and monthly average wave period (orange). Third: Hourly wave direction in degrees from north (blue) and average monthly wave period (orange). Fourth: Volumetric changes from DOD results at Saunton and Northam plotted on the date of the latter survey date. Dashed red lines indicate each Lidar survey date. Oceanographic data from Bideford Bay buoy was only available from June 2009. Data was provided by NNRCMP (2023).

Declaration of Interest Statement

Declaration of interests

☐The authors declare that they have no known competing financial interests or personal relationships that could have appeared to influence the work reported in this paper.

☒The authors declare the following financial interests/personal relationships which may be considered as potential competing interests:

Owen James reports financial support was provided by Natural Environment Research Council.